Proposal for the J-PARC 30-GeV Proton Synchrotron:

${}^{3}_{\Lambda}$H and ${}^{4}_{\Lambda}$H mesonic weak decay lifetime measurement with ^{3,4}He(K^-, π^0)${}^{3,4}_{\Lambda}$H reaction

H. Asano[1], X. Chen[4], A. Clozza[6], C. Curceanu[6], R. Del Grande[6], C. Guaraldo[6], C. Han[4,1], T. Hashimoto[3], M. Iliescu[6], S. Ishimoto[2], K. Itahashi[1], M. Iwasaki[1], Y. Ma[1], M. Miliucci[6], S. Okada[1], H. Outa[1], K. Piscicchia[6,8], F. Sakuma[1], M. Sato[2], A. Scordo[6], D. Sirghi[6,7], F. Sirghi[6,7], S. Suzuki[2], K. Tanida[3], T. Yamaga[1], X. Yuan[4], P. Zhang[4], Y. Zhang[4], H. Zhang[5]

[1]RIKEN, Wako, 351-0198, Japan
[2]High Energy Accelerator Research Organization (KEK), Tsukuba, 305-0801, Japan
[3]Japan Atomic Energy Agency, Ibaraki 319-1195, Japan
[4]Institute of Modern Physics, Gansu 730000, China
[5]School of Nuclear Science and Technology, Lanzhou University, Gansu 730000, China
[6]Laboratori Nazionali di Frascati dell INFN, I-00044 Frascati, Italy
[7]Horia Hulubei National Institute of Physics and Nuclear Engineering (IFIN-HH), Magurele, Romania
[8]CENTRO FERMI - Museo Storico della Fisica e Centro Studi e Ricerche “Enrico Fermi”, 00184 Rome, Italy

Executive Summary

Three recent heavy ion experiments (HypHI, STAR and ALICE) announced surprisingly short lifetime for ${}^{3}_{\Lambda}$H mesonic weak decay (MWD), which is difficult to interpret given the fact that ${}^{3}_{\Lambda}$H is a very loosely bound system. It will be very interesting to study this issue with a different experimental approach. We propose a direct measurement for ${}^{3}_{\Lambda}$H hypernucleus MWD lifetime with ~20% resolution; ${}^{4}_{\Lambda}$H hypernucleus lifetime will also be measured as a feasibility test for our experimental approach. The major parameters of this experiment are summarized below:

Reaction	:	^{3,4}He(K^-, π^0)${}^{3,4}_{\Lambda}$H reaction
Secondary beam	:	1.0 GeV/c K^-
Beam line	:	K1.8BR
Target	:	liquid ^{3}He and ^{4}He
Detector	:	Cylindrical Detector System (CDS) and PbF_2 γ-ray calorimeter
Beam time	:	3 days for detector commissioning
	:	50 kW $\times$ 5 weeks for production run (1 week for ${}^{4}_{\Lambda}$H; 4 weeks for ${}^{3}_{\Lambda}$H)

Contents

1 Introduction and physics motivation

As a very loosely bound system, Hypertriton($^3_\Lambda$H, B_Λ=130±50 keV[1]) is expected to possess a similar lifetime as free Λ hyperon (τ =263.2±2.0 ps). For instance, high precision few-body calculation shows that Λ hyperon is separated by ∼10 fm from np-pair(deuteron) inside $^3_\Lambda$H[2]. However, three heavy ion experiments(STAR[3], HypHI[4] and ALICE[5]) found surprisingly short lifetime for $^3_\Lambda$H in their measurements. This situation is summarized in Table1.

Collaboration	Experimental method	$^3_\Lambda$H lifetime [ps]	Release date
STAR	Au collider	142^{+24}_{-21}(stat.)±29(syst.)	2018
ALICE	Pb collider	181^{+54}_{-39}(stat.)±33(syst.)	2016
HypHI	fixed target	183^{+42}_{-32}(stat.)±37(syst.)	2013

Table 1: Summary of recent measurements on $^3_\Lambda$H lifetime.

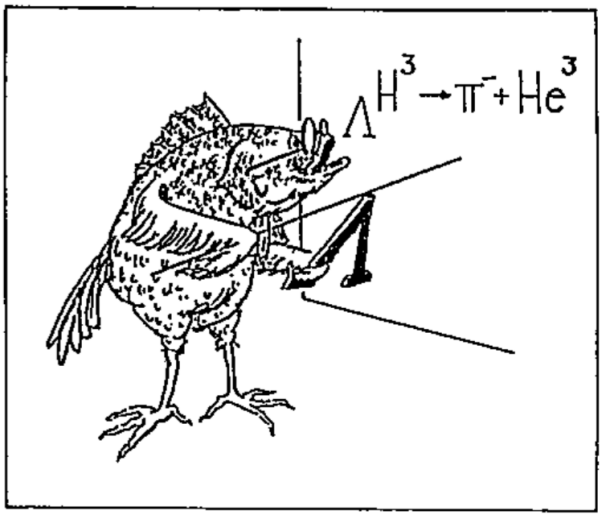

Figure 1: Neither fish nor fowl?[6]

This puzzling situation can be illustrated with Fig.1[6]. In order to shed light on this puzzling issue, we propose to measure $^3_\Lambda$H mesonic weak decay lifetime($^3_\Lambda$H→^{3}He + π^-) with ^{3}He(K^-, π^0)$^3_\Lambda$H production reaction. The advantage of this approach is that it allows us to carry out a direct lifetime measurement, which is different from the heavy ion experiments listed above. Data analysis technique is also established during previous KEK weak decay experiments [7][8]. On the other hand, the involvement of π^0 detection makes the reconstruction of hypernuclear ground state with missing mass method very difficult. Our solution is to construct a hadron blind γ-ray calorimeter to tag high energy π^0 events in very forward angle, which corresponds to Λ hyperon production with small recoil momentum. The yield of $^3_\Lambda$H hypernucleus can be enhanced by this event selection condition and result in a relatively good signal to background ratio. The momentum of π^- emitted from $^3_\Lambda$H mesonic weak decay at rest will be mono-chromatically distributed around 114.3 MeV/c because there is only one quantum state for this decay channel. We can identify the $^3_\Lambda$H events by selecting this peak on the delayed π^-

momentum spectrum. The background suppression can be achieved by subtracting the time distribution of the neighboring π^- in momentum spectrum as described in [8].

The same idea can be applied to the ${}^{4}_{\Lambda}$H hypernucleus production and its mesonic weak decay measurement because it shares the same experimental setup except the target material. The ${}^{4}_{\Lambda}$H MWD lifetime has been measured by [8] with ($K^-_{stopped}$, π^0) reaction, which will be used as a reference channel to test the performance of our approach.

2 Production method

With a simple phenomenological model, the production of Λ hypernucleus can be treated as a two-step process. First, a Λ hyperon is generated by one of the reactions listed in Fig.2; then the Λ hyperon has to be combined with the rest of nucleus described by a parameter called *sticking probability*. Qualitatively, Λ hyperon with smaller recoil momentum has larger *sticking probability*, which can be used as a guideline for hypernucleus production estimation. This argument is particularly true for *s-shell* hypernucleus because there is only one bound state for Λ hyperon in *s-orbit* and any $\Delta p \geq 200$ MeV/c reaction will cause $\Delta l = 1$ transition. Therefore, we plan to employ ^{3,4}He(K^-, π^0)${}^{3,4}_{\Lambda}$H reaction to populate ${}^{3,4}_{\Lambda}$H for their lifetime measurements because of the small recoil momentum among all three production channels.

In an ideal experimental setup, one can set the K^- beam momentum to be ∼0.5 GeV/c because the populated Λ hyperon will have no recoil momentum, which is often cited as *magic momentum*. However, it is difficult to prepare K^- beam with such a low momentum because of the K^- decay during transportation. In addition, the Λ hyperon production cross section is relatively low at this K^- beam momentum. A more common choice for Λ hypernucleus production with K^- beam is p_{K^-}≥0.75 GeV/c. The current K^- intensity at J-PARC K1.8BR as a function of beam momentum is given in Fig.3[9]. On the other hand, hyperon production cross section for p(K^-, π)Λ(Σ) elementary process as a function of K^- beam momentum when the projectile π meson comes out at 0 degree is given Fig.4[10]. By combining the K^- beam intensity and hyperon production cross section, a *figure of merit* can be obtained as shown in Fig.5. Taking into account the Λ to Σ ratio and Λ hyperon recoil momentum, our best choice is to perform the experiment at p_{K^-}∼1.0 GeV/c, which is used through out this proposal.

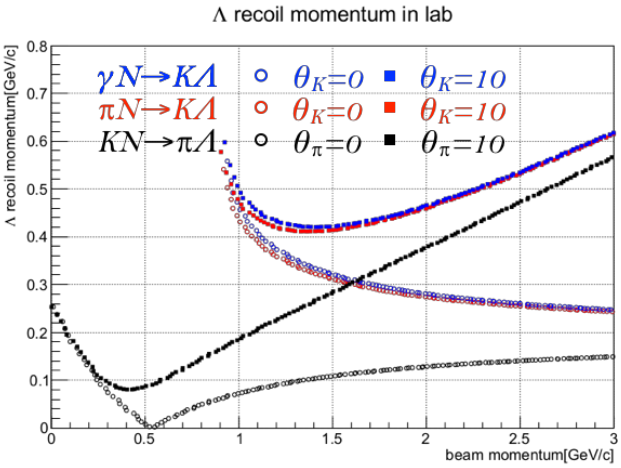

Figure 2: Recoil momentum of Λ hyperon from three different production method; p(K^-, π^0)Λ reaction has the lowest recoil momentum.

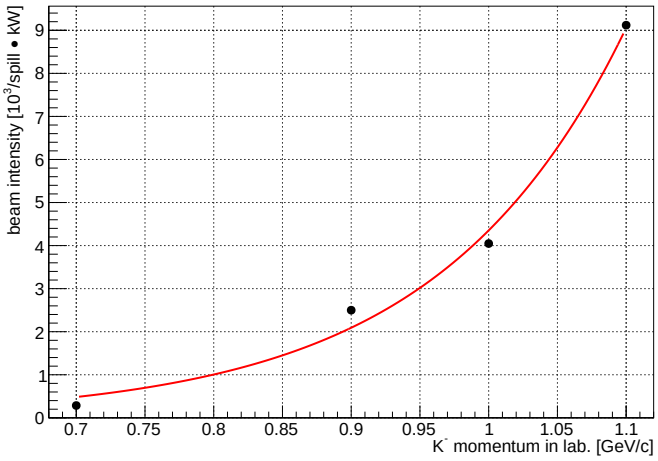

Figure 3: K^- beam intensity at K1.8BR beam line of J-PARC.

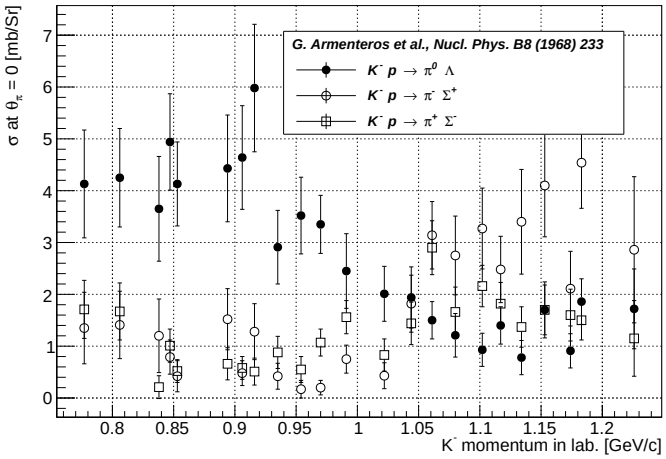

Figure 4: Production cross section for p(K^-, π)Λ,Σ reaction[10].

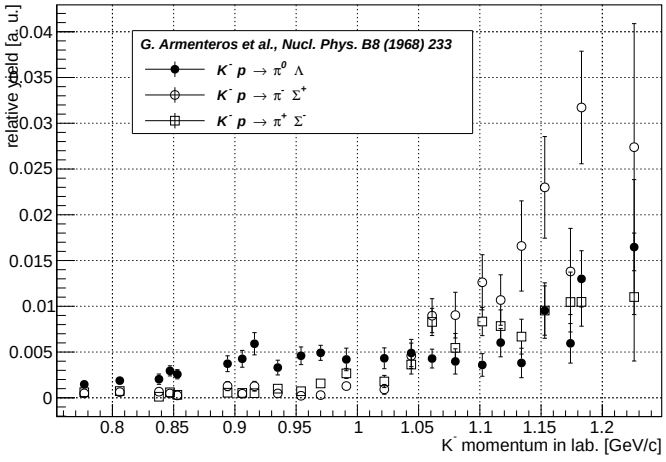

Figure 5: Figure of merit by combining K^- beam intensity and production cross section.

3 Production cross section estimation for ^{3,4}He(K$^-$, π^0)$^{3,4}_{\Lambda}$H process

The production cross section data for ^{3,4}He(K$^-$, π^0)$^{3,4}_{\Lambda}$H process at p_{K^-}=1.0GeV/c is not available. We will rely on a recent theoretical calculation as shown in Fig.6[11]. Quasi-free Λ hyperon production, which is the most dominant background, is estimated to be ~10 times more than hypertriton yield in the forward region. Because these Λ hyperons decay in-flight, the π^- momentum will be distributed between 80 ~ 140 MeV/c. So that the actual S/N ratio for π^- of 114 MeV/c signal region will be much better than 1/10. A GEANT4 based evaluation will be given in the Section 5 of this proposal. The production cross section of $^4_{\Lambda}$H is assumed to be three times of $^3_{\Lambda}$H.

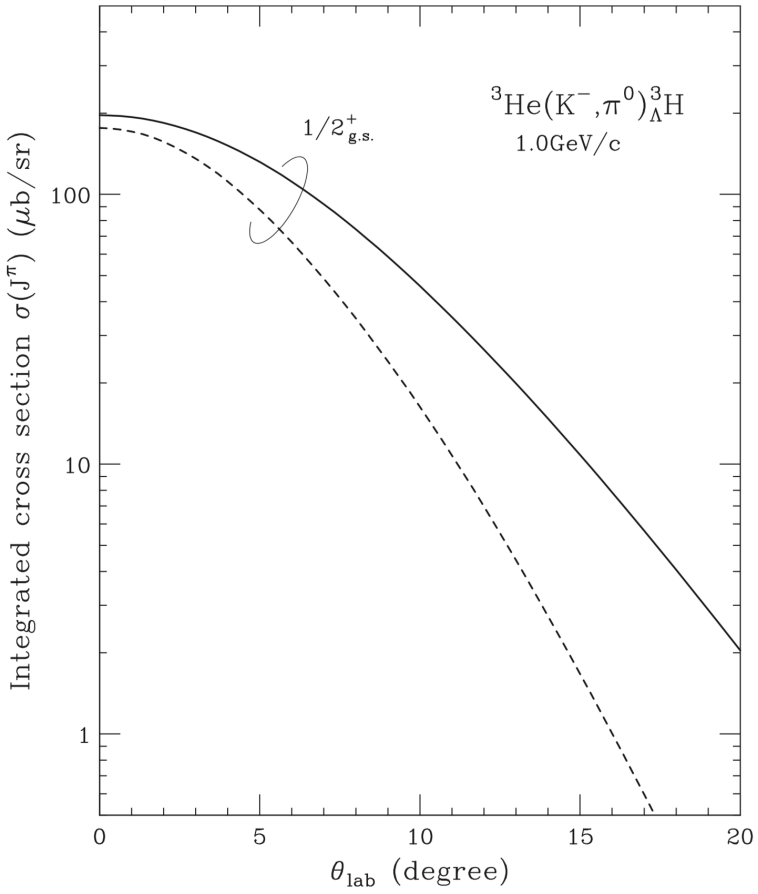

Figure 6: Calculated production cross section for ^{3}He(K$^-$, π^0)$^3_{\Lambda}$H reaction at 1.0 GeV/c.[11]

4 Experimental setup

The experimental concept is shown in Fig.7. A Cylindrical Detector System(CDS) used in J-PARC E15/E31 experiment is employed to capture the delayed π^- as a weak decay product from ${}^{3,4}_{\Lambda}$H hypernuclei[12]; a calorimeter is installed in the very forward region to tag fast π^0 meson along ~0 degree, which corresponds to small recoil momentum of Λ hyperon. Such a selection will improve the ratio between ${}^{3,4}_{\Lambda}$H and quasi-free Λ and Σ background. In the rest of this section, we will present the details of each detector component.

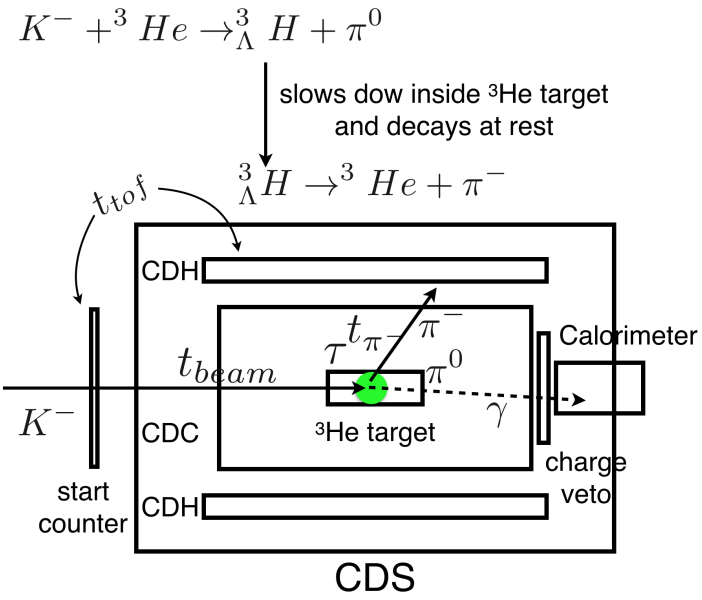

Figure 7: Schematic view of the experimental setup; Cylindrical Detector System(CDS) is used to capture delayed π^- particle from ${}^{3,4}_{\Lambda}$H weak decay; high-energy γ rays ($E_\gamma \geqslant 600$ MeV) are tagged with PbF_2 calorimeter.

4.1 γ-ray calorimeter

The most challenging task for the ${}^{3,4}_{\Lambda}$H production with (K^-, π^0) method is to identify the ground state of ${}^{3,4}_{\Lambda}$H hypernuclei, which involves the detection of π^0 particle. The outgoing π^0 decays into two γ rays almost immediately. The fast π^0 at the forward scattering angle boosts the decayed γ rays more forward than the slow π^0 events as illustrated in Fig.8. For π^0 with momentum of ~0.9 GeV/c and θ_{π^0}=0, the opening angle between decayed γ rays is centered at $\pm 8^0$. By covering the 0^0 ~8^0 region of polar angle, we can tag the γ ray decayed from π^0 with higher energies.

One can expect very high background rate from the unreacted beam hitting on the forward γ-ray calorimeter. After searching for materials available on the market, we decide to use PbF_2 crystal as Cherenkov based γ-ray calorimeter. Table2 summarizes related property of PbF_2 crystal. As shown in Fig.9, the PbF_2 crystals have a nice separation between pion and electron (and also γ) because of Cherenkov radiation mechanism [13]. As demonstrated by Fig.10, the PbF_2 crystal possesses good radiation hardness. For instance, an average of ~240 MeV will be deposited into $2.5\times2.5\times14$ cm^3 PbF_2 crystal by K^- beam particle of 1.0 GeV/c according to GEANT4 simulation. Assuming an intensity of 10^6/s, including π^- contamination, 4 Gy/day of radiation dose can be expected. The accumulated

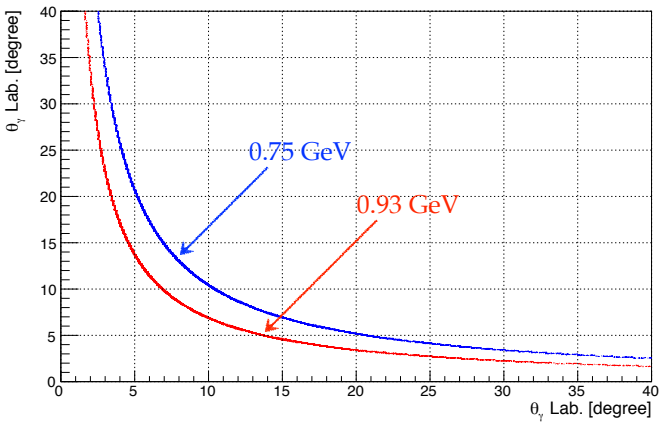

Figure 8: Angular correlation of γ rays decayed from π^0 with different momentum; upper curve is for p_{π^0} = 0.75 GeV/c; lower curve is for p_{π^0} = 0.93 GeV/c.

radiation dose during one month of data taking will be ~100 Gy, which will not have any significant performance degradation according to Fig.10 [13]. In addition, it is found that the PbF_2 can be recovered from radiation damage by exposed to light source of 365 nm wave length [13]. PbF_2 crystal also generates very fast signal with duration of ~20 ns because of its Cherenkov nature.

In the present design, we will use a 5 by 5 (25 pieces) PbF_2 segments with $2.5\times2.5\times14$ cm^3 dimension, which costs ~1k USD per crystal. Total budget including photon sensor and readout electronics is ~50k USD. Our funding application was approved in 2017 and the construction of γ-ray calorimeter is in progress.

Crystal	Radiation length	Moliere radius	Density	Cost[1]
PbF_2	0.93 cm	2.22 cm	7.77 g/cm^3	12 USD/cc

Table 2: Summary of PbF_2 crystal property.

[1] Unofficial quotation from SIC, CAS, Shanghai, China.

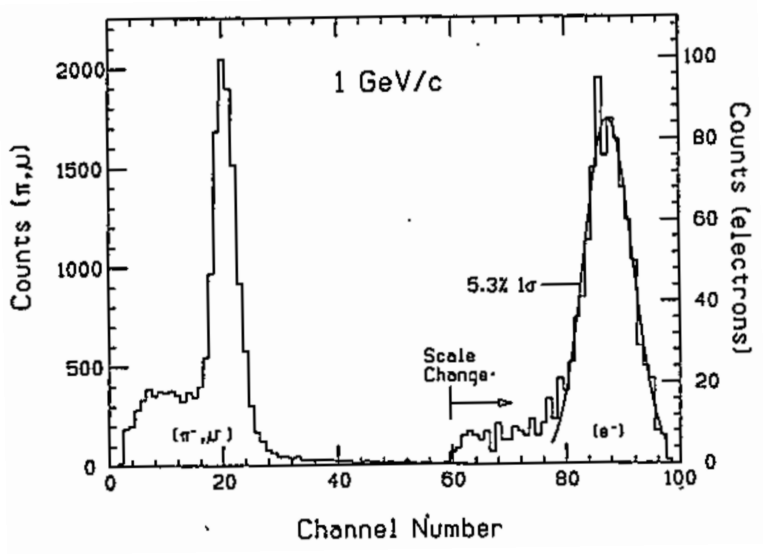

Figure 9: Light yield for 1.0 GeV/c pion and electron [13].

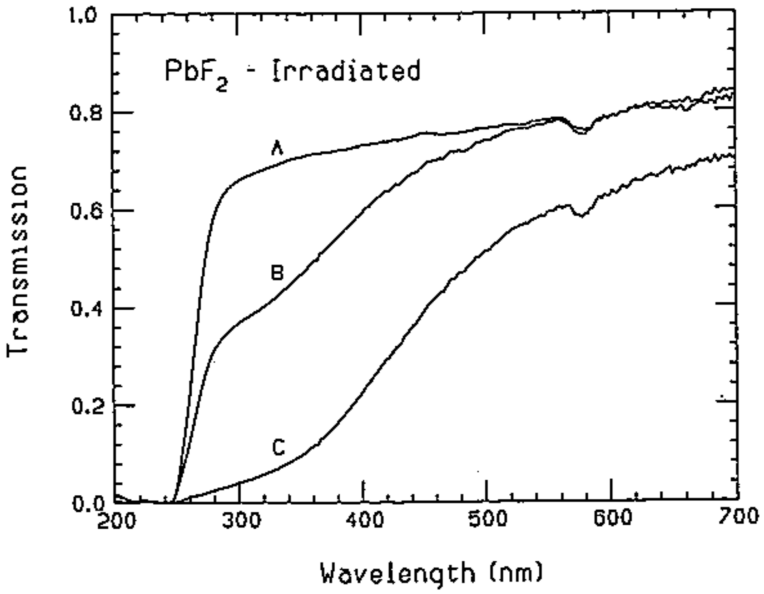

Figure 10: Effects of radiation dose on PbF_2 transmission: (A) is before radiation; (B) after 3×10^5 rad of neutron and 1×10^5 rad of γ rays; (C) after 3×10^6 rad of neutrons and 1×10^6 rad of γ rays [13].

4.2 π^- tracker

The produced ${}^{3,4}_{\Lambda}$H hypernucleus partially (~25% and ~50%, respectively) decays into ^{3,4}He and π^-, whose lifetime will be derived by the proposed experiment. If the ${}^{3,4}_{\Lambda}$H hypernuclei decay at rest, the π^- meson will have a well defined momentum of 114.3 and 133 MeV/c, respectively. The actual π^- distribution will be smeared out slightly because of the ${}^{3,4}_{\Lambda}$H in-flight decay. As can be seen in Appendix A, the recoiling ${}^{3,4}_{\Lambda}$H will be stopped within ~200 ps (or, ~1 mm) due to stopping effect inside the target. As one can easily estimate, for ${}^{3,4}_{\Lambda}$H hypernuclei, the in-flight decay effect for π^- is very limited because of the slow velocity of the recoiling mother particle. This observation is confirmed by our simulation in Section 5.

The proposed experiment is, in principle, a semi-inclusive measurement. The momentum resolution for π^- is the key factor for a successful identification for the production of ${}^{3,4}_{\Lambda}$H hypernuclei. We will use Cylindrical Detector System (CDS) originally designed for J-PARC E15 experiment for its demonstrated good performance. The CDS consists of a solenoid magnet, Cylindrical Drift Chamber (CDC) and a hodoscope made of plastic scintillator (CDH). For details, please refer to [12]. The momentum resolution of CDS is given in Fig.11, which is obtained with 0.7 T magnetic field[14]. The transverse momentum resolution for the interested region (p_{π^-}=114 MeV/c) is as good as ~1.5%. For π^- momentum lower than 110 MeV/c, the resolution becomes worse rapidly because of the energy loss of charged π^- inside target materials. This can be improved by correcting for the energy loss inside the CDS. According to our simulation, a total momentum resolution of ~2% can be achieved without major modification of the current setup.

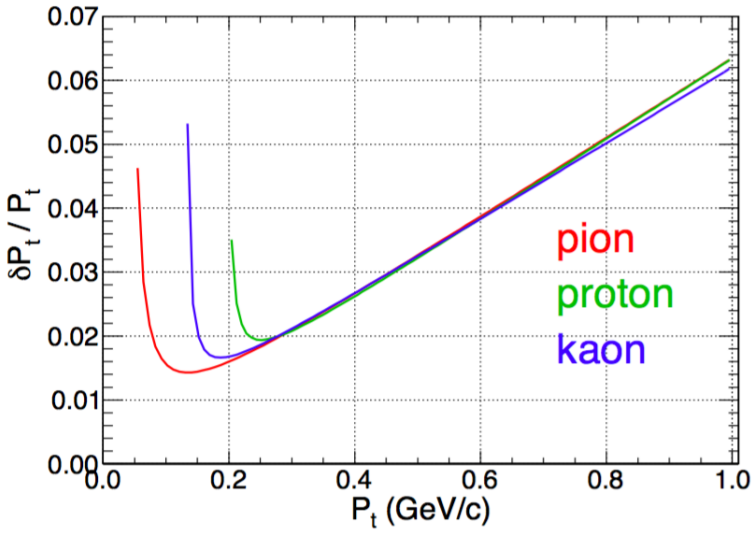

Figure 11: Momentum resolution of CDS [12].

5 Simulation and performance estimation

5.1 Simulation setup and event selection

The current simulation setup is based on the package prepared for E15 collaboration with a detailed description for magnetic field, material budget and detector resolution. The reliability of the simulation package has been demonstrated by E15 data analysis. The simulation configuration is shown in Fig.12. A calorimeter based on realistic PbF2 crystal property is constructed and used to select the forward γ-ray together with a charge veto counter placed in front of it. The liquid ^{3,4}He target system including target cell and vacuum chamber materials are all included in the simulation setup. The Cylindrical Drift Chamber (CDC) is also described in a very detailed way by implementing chamber wires and chamebr gas. The magnetic field used in the simulation is based on a calculated field map with TOSCA.

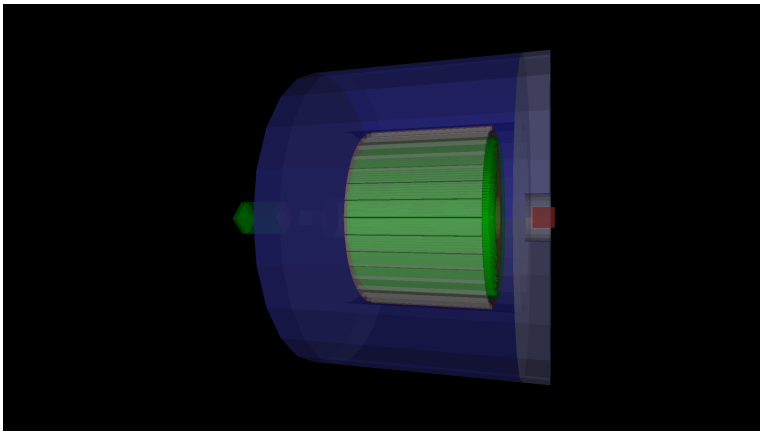

Figure 12: GEANT4 simulation setup based on package prepared by E15 collaboration; the block in red on the right side is the calorimeter block with PbF2 crystal; the barrel in green is for CDC tracking chamber; blue region is for the CDS iron yoke.

The generated simulation data is analyzed with offline analyzer, which has been used to obtain several published physical results for E15 data. The event selection criteria is outlined as followings:

- IH hit == 1
- DCA distance $\leq$ 0.5 cm
- CDS charged track == 1
- dE veto counter $\leq$ 0.2 MeV
- dE PbF2 calorimeter $\geq$ 600 MeV
- 0.0 GeV/c^2 $\leq$ mass $\leq$ 0.3 GeV/c^2
- reaction vertex within target volume

After fixing simulation routine and event selection condition, we optimize the experimental setup by adjusting calorimeter position. As can be seen from Fig.13, $^{3}_{\Lambda}$H bound state is mostly populated with very small π^0 scattering angle. This implies that a smaller π^0 acceptance in forward direction improves signal to noise ratio. However, we have to balance between a better S/N and minimization of statistical

fluctuation. Fig.14 shows the results of S/N and signal statistics at different calorimeter positions. We decide to install the calorimeter 70 cm down stream from the target center.

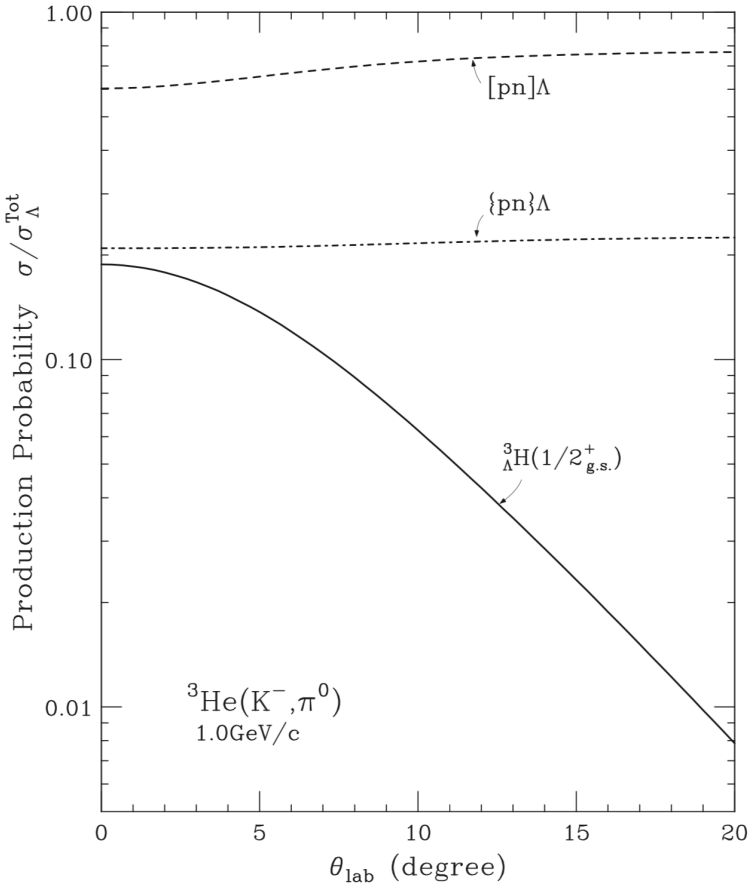

Figure 13: The relative yield between $^3_\Lambda$H bound state and quasi-free state calculated by Prof. Harada[11].

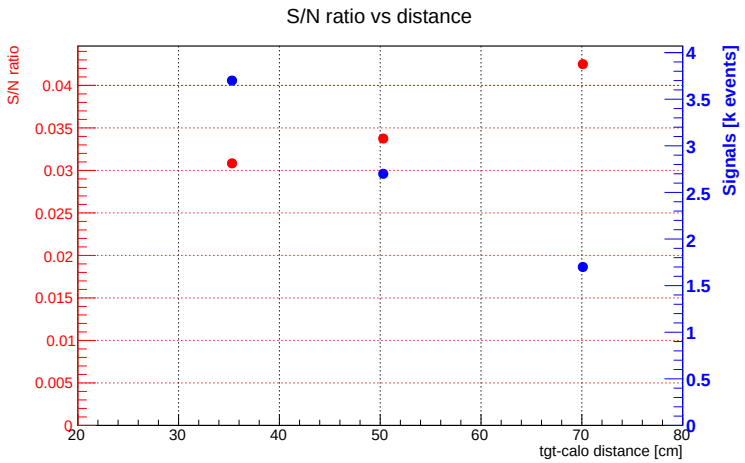

Figure 14: The S/N and signal statistics at different distances between target and calorimeter.

5.2 $^{3,4}_{\Lambda}$H yield estimation

The yield of $^{3}_{\Lambda}$H has been summarized in Table 3. The location of γ-ray calorimeter plays important role in the signal yield estimation because of the π^0 acceptance strongly depends on the distance between calorimeter and target. However, one can not leave the calorimeter very close to the target because of the large material budget of PbF_2 crystal causes serious contamination inside the CDS spectrometer. As described in the previous section, we suppose the calorimeter is installed 70 cm down stream from the target center.

Parameter	Value	Yield
$^{3}_{\Lambda}$H integrated cross section	$\overline{\sigma}_{0\sim20}$ = 0.0126mb	
^{3}He target(10 cm)	A=$\frac{1}{3}\times0.08$g/cm$^3\times10$cm$\times6.02\times10^{23}=1.6\times10^{23}$/cm^2	
K^- at 1.0 GeV/c(4 weeks)	B=$2\times10^5/5.2$s$\times3600\times24\times28=9\times10^{10}$	
Total yield	$\overline{\sigma}_{0\sim20}\times$A$\times$B	1.8×10^5
$^{3}_{\Lambda}$H$\rightarrow\pi^-$ branching ratio	0.25	4.5×10^4
Beam acceptance & DAQ eff.	~0.5	2.2×10^4
π^0 & π^- acceptance & event selection	6%	1.3×10^3

Table 3: $^{3}_{\Lambda}$H Yield estimation.

Based on the calculated production cross section for $^{3}_{\Lambda}$H and expected luminosity, we can foresee 2.2×10^4 signal events with 4 weeks beam time. These 2.2×10^4 $^{3}_{\Lambda}$H signal events are generated following the calculated differential cross section given in Fig.6 as input for GEANT4 simulation. During the generation of signal events, K^- beam emittance and momentum bite are also taken into account as illustrated in Fig.15. Populated $^{3}_{\Lambda}$H with recoiling momentum slows down according to SRIM simulation as described in Appendix A; $^{3}_{\Lambda}$H either decays in-flight or decays at rest by comparing its lifetime (assumed to be τ=0.2[ns]) with stopping time event by event. The π^- decayed from $^{3}_{\Lambda}$H after event selection is shown in Fig.16. As given in Table3, with the current setup, ~1.3k events can be collected with 4 weeks beam time. The π^- momentum distribution is slightly broadened due to in-flight decay. However, such in-flight decay will not effect the $^{3}_{\Lambda}$H lifetime measurement because the time dilation is only a very small fraction(~ 0.5%) compared with expected resolution(~ 10%).

As can be read from Table 3, ~1.3k $^{3}_{\Lambda}$H events will be collected with 4 weeks beam time. If we assume $\sigma_{^{3}_{\Lambda}H}/\sigma_{^{4}_{\Lambda}H}$ = 1/3 and taking into account the factor of 2 from two-body π^- decay branching ratio between $^{4}_{\Lambda}$H(b.r. = 50%) and $^{3}_{\Lambda}$H(b.r.=25%), one can expect 1.8k events from $^{4}_{\Lambda}$H hypernucleus with one week beam time.

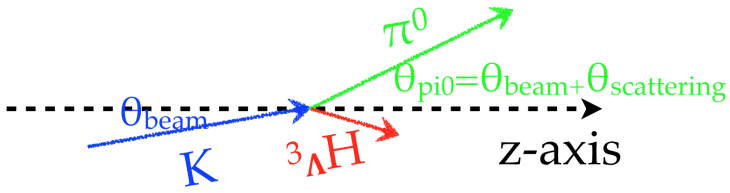

Figure 15: Illustration for the generation of ${}^{3}_{\Lambda}\mathrm{H}$ events.

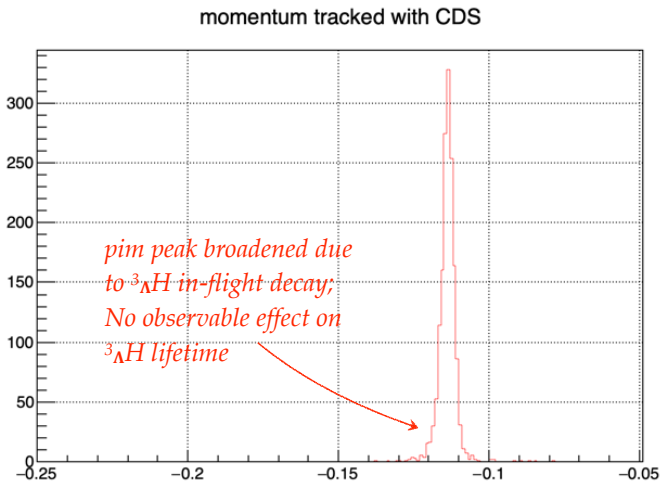

Figure 16: π^- signal events decayed from ${}^{3}_{\Lambda}\mathrm{H}$ after event selection; the momentum distribution is slightly broadened due to ${}^{3}_{\Lambda}\mathrm{H}$ in-flight decay.

5.3 Background estimation

In order to give a thorough investigation for the possible background π^- yield, we categorize the background events according to its origin: K^- beam in-flight decay induced background and K^- beam reaction induced background.

5.3.1 K^- decay induced background

Fig.17 shows the kinematics for $K^- \to \pi^- + \pi^0$ decay at 0.8 GeV/c and 1.0 GeV/c, respectively. In the shadowed region, π^- locates very closely to the expected signal(~ 114 MeV/c for ${}^{3}_{\Lambda}\mathrm{H}$ and ~133 MeV/c for ${}^{4}_{\Lambda}\mathrm{H}$); the accompanying π^0 is also boosted forwardly and yield the same trigger pattern as signals. Fig.18 clearly demonstrates the K^- decay and elastic scattering events in simulated data set. Fortunately, the CDS spectrometer only has acceptance at large scattering angles near target area as illustrated in Fig.19. One should notice that K^- beam with lower momentum contributes more in-flight decay background because of less Lorentz boost as illustrated by comparing green and magenta area in Fig.19: for 1.0 GeV/c K^- beam, the maximum decay angle is ~50 degree and for 0.8 GeV/c K^- beam, the maximum decay angle is ~70 degree. This is another reason we choose beam momentum to be 1.0 GeV/c. After requesting the forward π^0 by selecting a high energy γ-ray hitting on calorimeter and choosing reaction vertex within target volume, most of the background from K^- beam in-flight decay can be suppressed as can be seen in Fig.20.

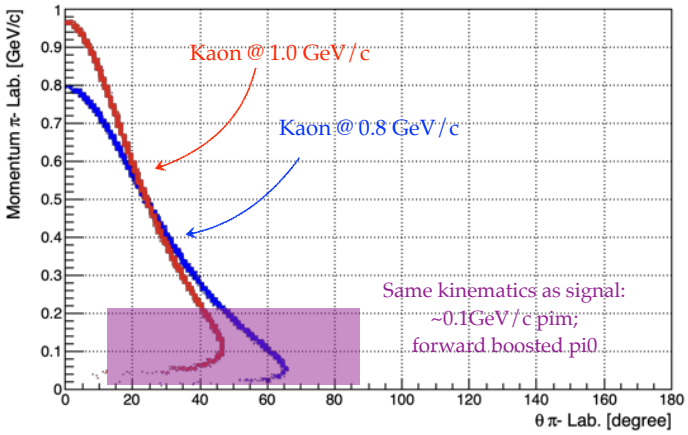

Figure 17: Kinematics for Kaon decays into two pions at 0.8 GeV/c and 1.0 GeV/c, respectively.

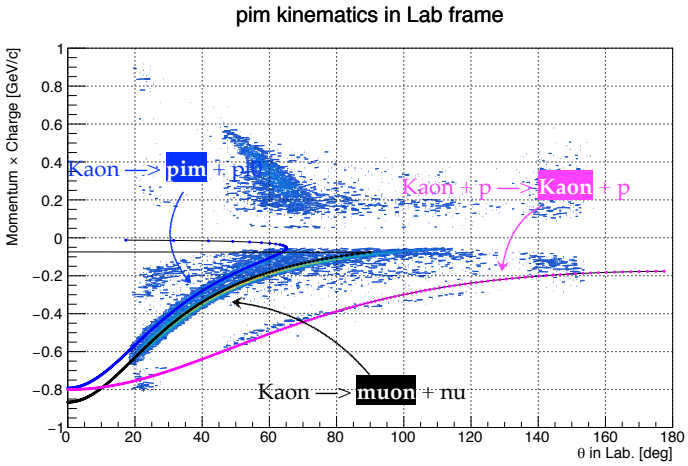

Figure 18: Inclusive π^-/μ^- background induced by 0.8 GeV/c K^- beam in-flight decay and elastic scattering before event selection. Eye guide line is based on phase space decay (reaction).

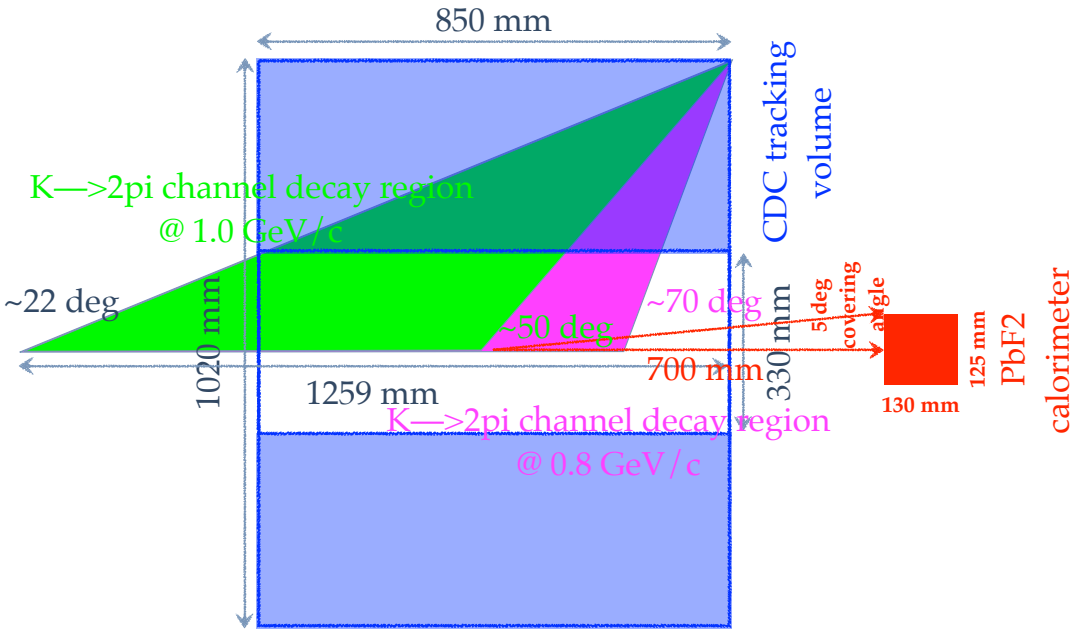

Figure 19: Schematic CDC acceptance: green (magenta) area is for the acceptance for K^- decay into two pions at 1.0 GeV/c (0.8 GeV/c).

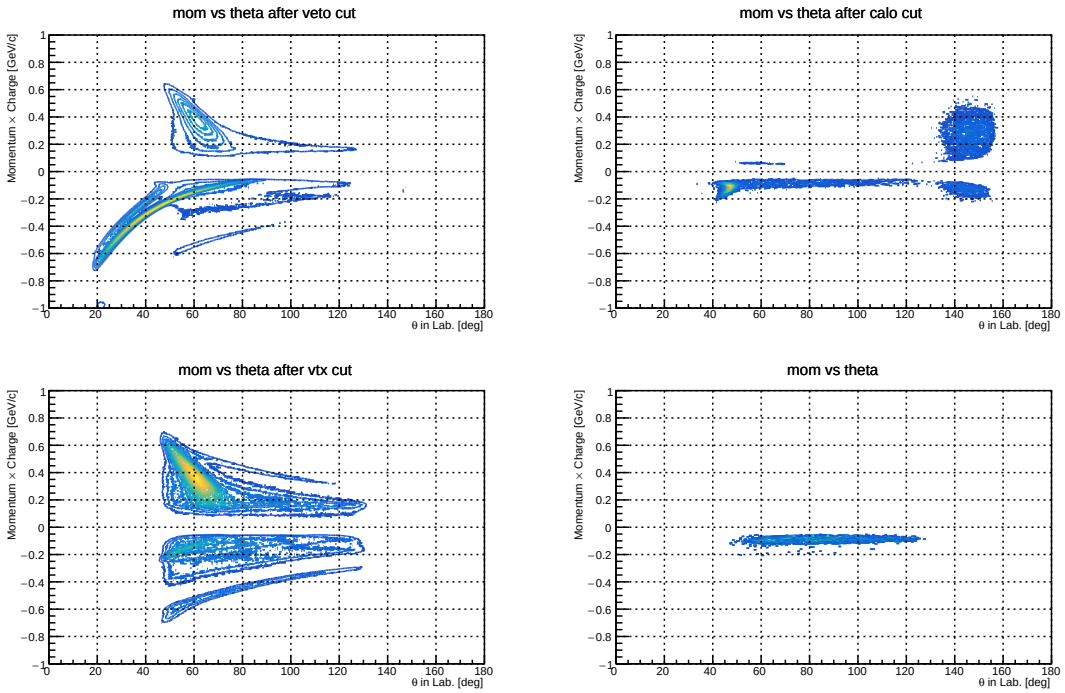

Figure 20: Background π^- from 1.0 GeV/c K^- beam bombarding ^{3}He target after various cutting conditions: upper left requesting veto counter dE≤0.2 MeV; upper right requesting calorimeter dE≥600 MeV; lower left requesting reaction volume within target region; lower right is obtained after applying all cutting conditions, π^- background due to in-flight decay can be effectively suppressed and only reaction induced background is left, which will be discussed in the next section.

5.3.2 K^- reaction induced background

As described in previous section and Appendix B, most contamination after event selection come from quasi-free Λ and $\Sigma^{-,0}$ production. To have a reliable estimation for the background yield, we performed GEANT4 simulation with 1.0 GeV/c K^- beam directly bombarding both liquid ^{3}He and liquid Hydrogen target for comparison. So that the GEANT4 built-in Hyperon production cross section can provide an order of magnitude estimation for the final background π^- spectrum. We artificially increased the density of liquid ^{3}He/Hydrogen target by a factor of ten (from 0.081 g/cm^3 to 0.81 g/cm^3). This modification allows us to simulate 10 hours experimental luminosity with three days computing time on a 40 core Linux server. The simulation data was analyzed with the cutting conditions listed in previous section. [2]

For the liquid ^{3}He target, we found some *unphysical* events probably due to some artifact caused by GEANT4 data model. For instance, there are several reactions with heavy ion involved generate π^- at precisely 0.10058 GeV/c regardless final products; another *unphysical* π^- peak shows up at 0.0880731 GeV/c. We obtained background events after fitting these *unphysical* peaks into a consinuous background. The final π^- background events are scaled by a factor of
24 hours $\times$ 28 days/10 hours simulated luminosity $\sim$ 67
to convert it into full luminosity. After applying cutting conditions, the final signal and background results are shown in Fig.21.

To cross check the background yield without the ambiguity caused by GEANT4 data model, we change target to 0.831g/cm^3 liquid Hydrogen and perform the same simulation/analysis tool chain. The equivalent luminosity for Hydrogen case can be obtained by taking into account the following effects:

- Shadowing effect: because cross section is proportional to $A^{2/3}$, the effective surface of ^{3}He is $\sim$2/3 of its nucleon number; For the artificial high density liquid hydrogen target, the proton number is 10 times of the number of nucleons in experimental ^{3}He target, which means 15 times of ^{3}He cross section in experiment;

- Isospin effect: as can be read from Appendix B, Kp $\rightarrow \pi^0\Lambda \rightarrow \pi^0\pi^- p$ $\sim$3 and Kn $\rightarrow \pi^0\Sigma^- \rightarrow \pi^0\pi^- n$ $\sim$1; For Hydrogen and ^{3}He target with the same number of nucleons, the relative reaction probability is related by $\frac{prob.Hydrogen}{prob.He3} = \frac{3+3+3}{3+3+1} = \frac{9}{7}$.

In summary, the effective luminosity of hydrogen target (0.831g/cm^3) is 15$\times$9/7 $\sim$20 of experimental ^{3}He target. Simulation results for one hour of 0.831g/cm^3 Hydrogen was scaled by a factor of
24 hours $\times$ 28 days/20 hours simulated luminosity $\sim$ 33
to account for 4 weeks beam time. The final signal and background π^- spectrum survived all event selection conditions is shown in Fig.22.

The difference between Fig.21 and Fig.22 is mainly caused by the contribution from Σ^- decay channel[3], which is not included in Fig.22 because of the absence of neutron. Nevertheless, one can expect $\sim$20% of π^- in Fig.22 spread to the left (high momentum) side of pim momentum spectrum due to Σ^- decay events which can not be seen with the current K^- proton configuration. So that the actual background shape should fall in between these two cases. We would like to emphasize that even for the

[2] In the offline analysis, we request γ-ray energy $\geq$600 MeV from calorimeter and a single minus charged CDS track with mass in-between 0.0 GeV/c^2 and 0.3 GeV/c^2. The mass calculated as the TOF between reaction vertex and CDH hit position doesn't include the weak decay lifetime effect. Therefore, the calculated mass is shifted to the heavier side by $\sim$50 MeV/c^2. As far as the PID can separate π^- from K^-, this mass shift will not cause serious problem in the energy loss correction and event selection.

[3] K^-+n$\rightarrow\Sigma^-\pi^0\rightarrow$n+$\pi^-$+$\pi^0$

more challenging case shown in Fig.22, the π^- signal region can still be identified. The S/N for both cases varies from 0.2~0.3 in a comparable way, which allows us to derive ${}^{3}_{\Lambda}\mathrm{H}$ with reasonable resolution as will be presented in the next section. For a further reference, Fig.23 shows estimated signal and background with Prof. Harada's calculation given by Fig.13. The contamination from prompt hadron reaction is not included. The signal has been scaled to achieve 1k statistics as obtained from dedicated signal simulation described in previous section; the quasi-free Λ events are also scaled based on relative cross section between Hypertriton and Λ.

From the simulation with Hydrogen target, it has been confirmed that most π^- events passing cutting conditions in Fig.22 are decayed from slowly recoiling Λ with ~0.1 MeV/c momentum and it is almost free from prompt hadronic reaction contamination. By assuming the same forward production of Σ^- as Λ, we found that the π^- decayed from Σ^- distribute from 140 MeV/c to 260 MeV/c, which is shifted from the signal region of ${}^{3}_{\Lambda}\mathrm{H}$ (114 MeV/c) and will not effect its lifetime derivation. This is a favourable situation for our goal: we just need to verify if there are short lifetime components (assuming ${}^{3}_{\Lambda}\mathrm{H}$ does have a shorter lifetime as reported) among long lived Λ hyperon.

It is also worth to address that the S/N for ${}^{4}_{\Lambda}\mathrm{H}$ case will be much better because the π^- peak position is away from the contamination and the background yield will be a quarter of the ${}^{3}_{\Lambda}\mathrm{H}$ case. Therefore, we could effectively study the feasibility in one week beam time with ${}^{4}\mathrm{He}$ target and pin down the uncertainty for the π^- background shape. We would also call the attention of referee that the uncertainty of background shape is mainly due to the lack of semi-inclusive data with forward π^0 as final product. A *quick* measurement with ${}^{4}\mathrm{He}$ target will help us to establish a new method for the study of neutron-rich hypernucleaus with ${}_{Z}\mathrm{A}(\mathrm{K}^-, \pi^0){}_{Z-1}\mathrm{A}$ reaction.

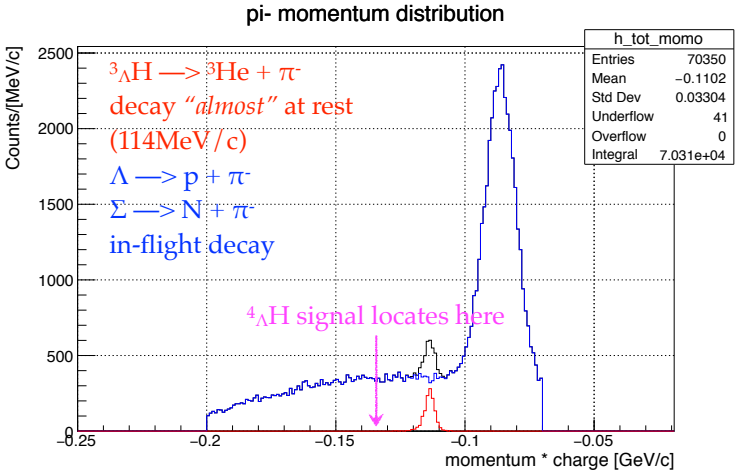

Figure 21: π^- momentum distribution: peak in red is from ${}^{3}_{\Lambda}\mathrm{H}$ decay, blue curve shows π^- from other hyperon weak decay channels based on GEANT4 simulation with liquid ${}^{3}\mathrm{He}$ target.

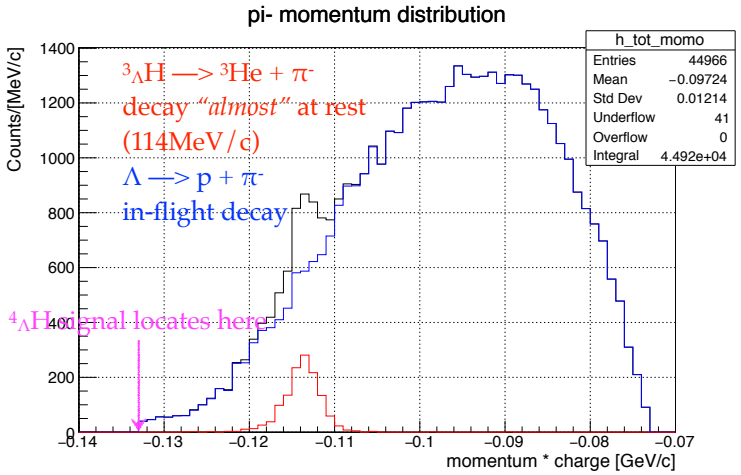

Figure 22: π^- momentum distribution: peak in red is from $^3_\Lambda$H decay, blue curve shows π^- from other hyperon weak decay channels based on GEANT4 simulation with liquid Hydrogen target.

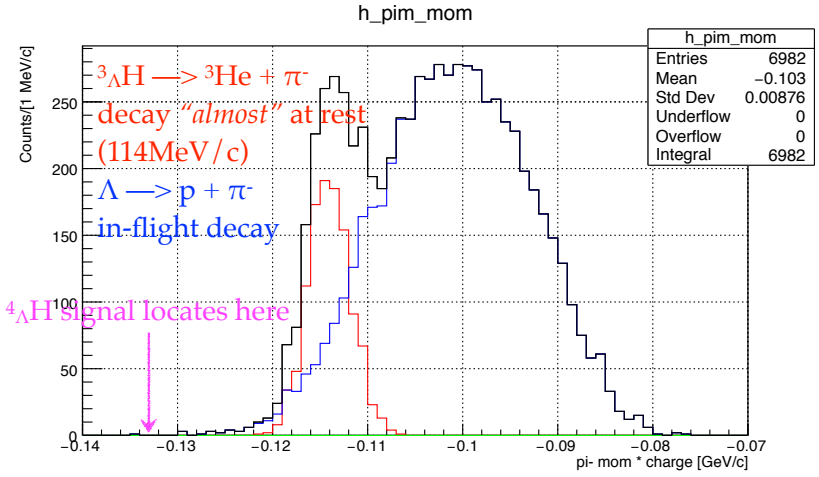

Figure 23: π^- momentum distribution: peak in red is from $^3_\Lambda$H decay, blue curve shows π^- from other hyperon weak decay channels based on theoretical calculation given in Fig.13[11].

5.4 Lifetime determination

As illustrated in Fig.7, the relation between ${}^{3,4}_{\Lambda}$H lifetime and experimental observable is

$$T_{CDH} - T_0 = t_{beam} + t_{\pi^-} + \tau_0, \tag{1}$$

where $T_{CDH} - T_0$ is the TOF between t0 and CDH counter, t_{beam} is the K^- TOF between t0 counter and reaction vertex, t_{π^-} is the TOF of π^- between decay vertex and CDH and τ_0 is the ${}^{3,4}_{\Lambda}$H lifetime to be derived from the experiment. The value of t_{beam} and t_{π^-} can be calculated by CDS tracking[4]. In the data analysis, we have assumed reaction vertex is the same as decay vertex and defined as the closest crossing point between K^- beam and π^- tracks. This approximation will cause a sub-centimeter error due to ${}^{3,4}_{\Lambda}$H recoiling, which is comparable with the CDS vertex resolution. This effect has been accumulated into the total time resolution of 200 ps. The τ_0 obtained this way is not the *exact* lifetime of ${}^{3,4}_{\Lambda}$H yet but the lifetime convoluted with CDS time resolution, which can be written as:

$$f(t) = \int_{-\infty}^{+\infty} e^{-(t-u)/\tau} R(u) du, \tag{2}$$

where $R(u)$ is the response function due to limited time resolution. This relation is used, in turn, to fit the π^- time distribution and derive the lifetime.

In order to give a more realistic estimation for achievable ${}^{3}_{\Lambda}$H lifetime resolution, we use the more challenging results from Hydrogen target simulation as an example. The π^- time distribution in signal region (0.110 MeV/c$\leq P_{\pi^-} \leq$0.116 MeV/c) obtained by TOF and tracking analysis is shown in Fig.24. As can be seen from the Fig.24, there is large fluctuation due to the scaling of background statistics. We tried to overcome this problem be keeping the S/N and statistics obtained from simulation and generate two time distributions for both signal (τ = 200 ps) and background (τ = 260 ps), respectively. An experimental time resolution of 200 ps is also convoluted into the lifetime distribution. The generated time distribution for both signal and background are shown in Fig.25. Before fitting the data with with function $f(t)$, the response function resolution is fixed at σ = 200 ps and time origin is assumed to be perfectly aligned at time 0. In real data, the response function $R(u)$ can be obtained from prompt hadronic reactions and time alignment precision will determine the systematic error of the measurement, as will be given later. With all these preparations, a minimum Chi square fitting gives

$$\tau = 192 \pm 29\text{ps}, \tag{3}$$

where the ±29 ps is the statistical error. A quick estimation with signals statistics (∼1k) and time resolution of σ=200 ps gives $\sigma/\sqrt{1000}$ ∼10ps. The difference is due to the subtraction process introduces more fluctuation as shown in Fig.25. The systematic error is estimated by assuming a mis-alignment of time 0 during data analysis. A shift of ±20 ps due to mis-alignment results a systematic error of ±30 ps. In summary, given the challenging S/N with Hydrogen target simulation, we could expect a lifetime resolution of $\sigma_{stat.} \sim 30$ ps and $\sigma_{sys.} \sim 30$ ps, which is comparable with heavy ion results listed in Table1.

[4]For details of vertex reconstruction and velocity derivation with CDS, please refer to [12].

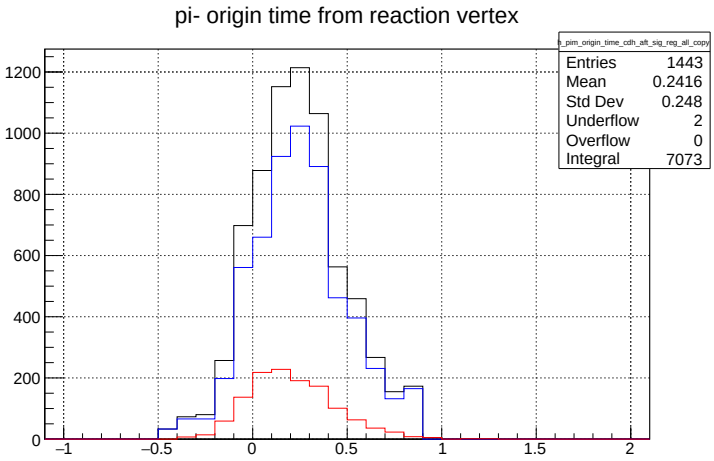

Figure 24: Time distribution of π^- after event selection: blue data points are background events from hyperon decay; red data points are ${}^{3}_{\Lambda}\mathrm{H}$ events from simulation.

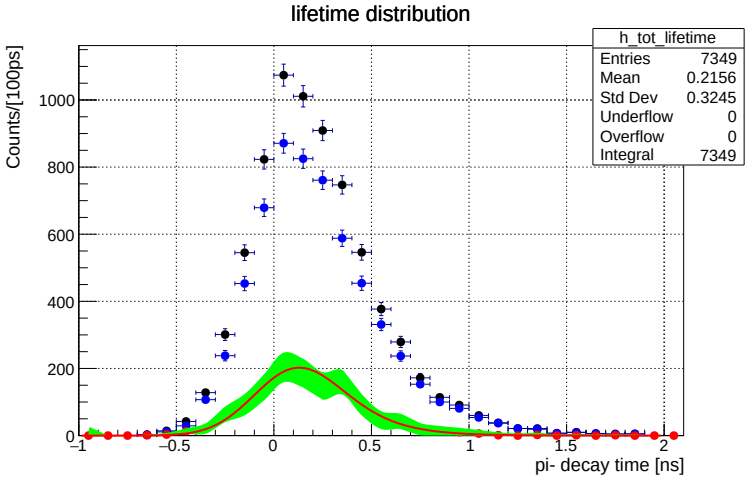

Figure 25: Generated time distribution of π^- with S/N and statistics obtained from simulation with Hydrogen target: blue data points are background events from hyperon decay; red data points are ${}^{3}_{\Lambda}\mathrm{H}$ events after subtracting background distribution.

6 Proposal timeline

6.1 Liquid ^{3}He target modification

The current E15 target system uses a large cylindrical vacuum chamber, which conflicts with the proposed PbF_2 calorimeter installation position. We have to modify the current design with a thinner vacuum pipe to allocate space for the calorimeter. There are feasible design experience from J-PARC E13 collaboration for us to follow. In principle, target modification can be finished in one year from now. The remaining ^{3}He purchased for E15 experiment can be used for our measurement.

6.2 PbF_2 calorimeter construction and commissioning

We received 30 pieces of PbF_2 crystals from SIC, CAS, Shanghai, China in Decembaer, 2018. We will assemble the crystals to construct γ-ray calorimeter. A test beam to study its performance and align the gain for each crystal is also in planing.

One of the possible challenges we need to verify is the particle flux into CDC due to the installation of PbF_2 calorimeter, which has a rather high density (7.7 g/cm^3). If there are too many CDC hits caused by δ-ray and γ-ray emitted from the calorimeter, the safe operation of CDC will become a problem. The simulation result with 1×10^6 K^- beam is shown in Fig.26. It seems that the CDC flux will only increase slightly if we install calorimeter at 70 cm from target center, which is represented by red curve in Fig.26. However, we need to verify the feasibility of this setup in the beginning of the beam time.

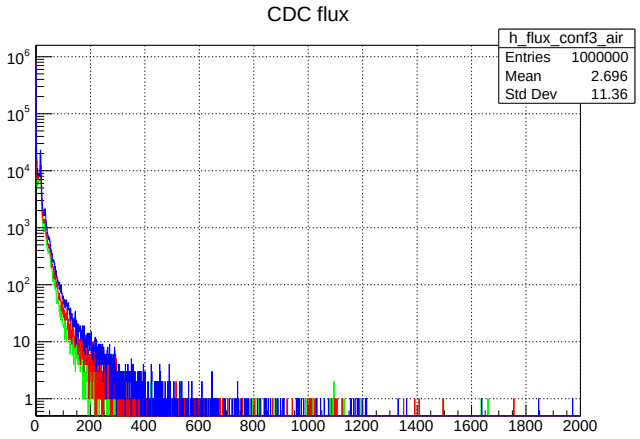

Figure 26: CDC hits flux distribution per event with different detector setup: W/O PbF_2 calorimeter (green), PbF_2 calorimeter located at 70 cm downstream of target center (red), PbF_2 calorimeter located at 30 cm of target center (blue).

7 Beam time request

Based on the estimation described in the previous sections, we require in total 38 days beam time with 50 kW beam power. The details for the beam time schedule is listed as:

Detector commissioning	:	3 days
${}^{4}_{\Lambda}$H production	:	7 days
${}^{3}_{\Lambda}$H production	:	28 days

References

[1] M. Juric *et al*., Nucl. Phys. B, **52**, 1, (1973)

[2] Private communication with Prof. E. Hiyama, (2016)

[3] L. Adamczyk *et al*., Phys. Rev. C, **97**, 054909, (2018)

[4] C. Rappold *et al*., Nucl. Phys. A, **913**, 170, (2013)

[5] ALICE collaboration, Phys. Lett. B, **754**, 360, (2016)

[6] M. Block *et al*., Proc. Int. Conf. Hyperfragments, 63, (1963)

[7] H. Bhang *et al*., J. Kor. Phys. Soc., **59**, 1461, (2011)

[8] H. Outa *et al*., Nucl. Phys. A, **547**, 109c, (1992)

[9] Private communication with Dr. F. Sakuma, (2016)

[10] G. Armenteros *et al*., Nucl. Phys. B, **8**, 233, (2012)

[11] Private communication with Prof. T. Harada, (2016)

[12] K. Agari *et al*., Prog. Theo. Exp. Phys., **02B011**, (2012)

[13] D.F. Anderson *et al*., Nucl. Inst. Meth. A, **290**, 385, (1990)

[14] T. Hashimoto, Doctor Thesis, University of Tokyo, (2013)

[15] www.srim.org

A $^{3}_{\Lambda}$H stopping time estimation

The recoiling $^{3}_{\Lambda}$H gradually stops inside liquid ^{3}He target before it decays. The stopping power in [MeV/mm] units for different kinetic energy of $^{3}_{\Lambda}$H is given in Fig.27 based on calculation with *SRIM*[**?**]. The stopping power in Fig.27 is fitted with a 4th order polynomial. This curve can be converted into stopping time and recoil momentum relation. The results is shown in Fig.28. We can read from Fig.28 that the $^{3}_{\Lambda}$H with $p \leq 0.2$ GeV/c($p \leq 0.3$ GeV/c) recoiling momentum will be stopped after ~150 ps(~400 ps). It implies that by selecting π^{-} event with long enough delay, the $^{3}_{\Lambda}$H hypernucleus is effectively decay at rest.

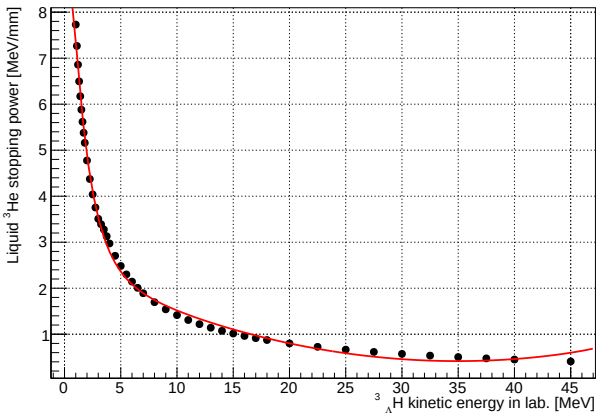

Figure 27: Stopping power of liquid ^{3}He target for recoiling $^{3}_{\Lambda}$H hypernucleus.

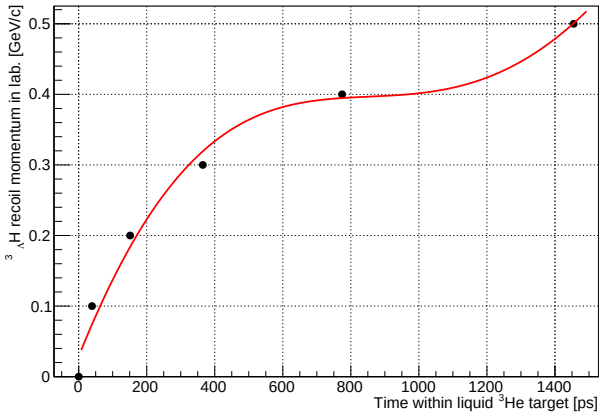

Figure 28: Slowing down of recoiling $^{3}_{\Lambda}$H hypernucleus within liquid ^{3}He target as a function of time.

B Background Survey

The survey for K^{-} related reaction channels as possible background are listed in Table 4[10]. The reactions involve a prompt π^{-} can be effectively suppressed by selecting delayed events[8]. Most con-

tamination after selecting fast π^0 and delayed π^- comes from quasi-free Λ and Σ^- production, which is used in this proposal to give a performance estimation.

Reaction(decay) and final states	Charged particle timing structure	Branching ratio	σ [mb/Sr] for p_{K^-}=0.9 GeV/c and θ_{π^0}=0
$K^- \, {}^3\mathrm{He} \rightarrow \pi^0 \, {}^3_\Lambda\mathrm{H} \rightarrow \begin{cases} \pi^0 \, \pi^- \, {}^3\mathrm{He} \rightarrow 2\gamma \, \pi^- \, {}^3\mathrm{He} \\ \pi^0 \, \mathrm{p} \, \mathrm{n} \, \mathrm{n}_s \rightarrow 2\gamma \, \mathrm{p} \, \mathrm{n} \, \mathrm{n} \end{cases}$	delayed π^- delayed p	?% ?%	?% ?%
$K^- \rightarrow \begin{cases} \pi^0 \mu^- \bar{\nu}_\mu \rightarrow 2\gamma \mu^- \bar{\nu}_\mu \\ \pi^0 \pi^- \rightarrow 2\gamma \pi^- \\ \pi^0 \pi^0 \pi^- \rightarrow 4\gamma \pi^- \end{cases}$	prompt μ^- prompt π^- prompt π^-	3.32% 20.92% 1.76%	Not included
$K^- \, \mathrm{p} \rightarrow \pi^0 \, \Lambda \rightarrow \begin{cases} \pi^0 \, \pi^0 \, \mathrm{n} \rightarrow 4\gamma \, \mathrm{n} \\ \pi^0 \, \pi^- \, \mathrm{p} \rightarrow 2\gamma \, \pi^- \, \mathrm{p} \end{cases}$	N. A. delayed π^-, p	35.8% 63.9%	4.5
$K^- \, \mathrm{p} \rightarrow \pi^0 \, \Sigma^0 \rightarrow \pi^0 \, \gamma \, \Lambda \rightarrow \begin{cases} \pi^0 \, \gamma \, \pi^0 \, \mathrm{n} \rightarrow 5\gamma \, \mathrm{n} \\ \pi^0 \, \gamma \, \pi^- \, \mathrm{p} \rightarrow 3\gamma \, \pi^- \, \mathrm{p} \end{cases}$	N. A. delayed π^-, p	35.8% 63.9%	0.36 (scaled)
$K^- \, \mathrm{p} \rightarrow \pi^- \, \Sigma^+ \rightarrow \begin{cases} \pi^- \, \pi^0 \, \mathrm{p} \rightarrow 2\gamma \, \pi^- \, \mathrm{p} \\ \pi^- \, \pi^+ \, \mathrm{n} \end{cases}$	prompt π^-, delayed p N. A.	51.57% 48.31%	0.9
$K^- \, \mathrm{p} \rightarrow \pi^+ \, \Sigma^- \rightarrow \pi^+ \, \pi^- \, \mathrm{n}$	N. A.	100%	Not included
$K^- \, \mathrm{n} \rightarrow \pi^- \, \Lambda \rightarrow \begin{cases} \pi^- \, \pi^0 \, \mathrm{n} \rightarrow 2\gamma \, \pi^- \, \mathrm{n} \\ \pi^- \, \pi^- \, \mathrm{p} \rightarrow 2\pi^- \, \mathrm{p} \end{cases}$	prompt π^- N. A.	35.8% 63.9%	Not included
$K^- \, \mathrm{n} \rightarrow \pi^- \, \Sigma^0 \rightarrow \pi^- \, \gamma \, \Lambda \rightarrow \begin{cases} \pi^- \, \gamma \, \pi^0 \, \mathrm{n} \rightarrow 3\gamma \, \pi^- \, \mathrm{n} \\ \pi^- \, \gamma \, \pi^- \, \mathrm{p} \rightarrow \gamma \, 2\pi^- \, \mathrm{p} \end{cases}$	prompt π^- N. A.	35.8% 63.9%	Not included
$K^- \, \mathrm{n} \rightarrow \pi^0 \, \Sigma^- \rightarrow \pi^0 \, \pi^- \, \mathrm{n} \rightarrow 2\gamma \, \pi^- \, \mathrm{n}$	delayed π^-	100%	0.9 (scaled)

Table 4: Survey for K^- + ^{3}He → forward π^0 + delayed π^-.